![remote sensing logo]

MDPI

A Satellite-Based Sunshine Duration Climate Data Record for Europe and Africa

Steffen Kothe *, Uwe Pfeifroth, Roswitha Cremer, Jörg Trentmann and Rainer Hollmann

Deutscher Wetterdienst, 63067 Offenbach, Germany; Uwe.Pfeifroth@dwd.de (U.P.);
Roswitha.Cremer@dwd.de (R.C.); Joerg.Trentmann@dwd.de (J.T.); Rainer.Hollmann@dwd.de (R.H.)
* Correspondence: Steffen.Kothe@dwd.de

Abstract: Besides 2 m–temperature and precipitation, sunshine duration is one of the most important and commonly used parameter in climatology, with measured time series of partly more than 100 years in length. EUMETSAT's Satellite Application Facility on Climate Monitoring (CM SAF) presents a climate data record for daily and monthly sunshine duration (SDU) for Europe and Africa. Basis for the advanced retrieval is a highly resolved satellite product of the direct solar radiation from measurements by Meteosat satellites 2 to 10. The data record covers the time period 1983 to 2015 with a spatial resolution of $0.05° \times 0.05°$. The comparison against ground-based data shows high agreement but also some regional differences. Sunshine duration is overestimated by the satellite-based data in many regions, compared to surface data. In West and Central Africa, low clouds seem to be the reason for a stronger overestimation of sunshine duration in this region (up to 20% for monthly sums). For most stations, the overestimation is low, with a bias below 7.5 h for monthly sums and below 0.4 h for daily sums. A high correlation of 0.91 for daily SDU and 0.96 for monthly SDU also proved the high agreement with station data. As SDU is based on a stable and homogeneous climate data record of more than 30 years length, it is highly suitable for climate applications, such as trend estimates.

Keywords: sunshine duration; satellite-based; climate monitoring; Meteosat

1. Introduction

Sunshine duration has been used for decades in many different applications. It is applied in sectors such as tourism, public health, agriculture and solar energy. There are several stations worldwide with measured time series of more than 100 years [1,2]. Thus, it is a well-known and easy-to-use parameter.

Current satellite-based data records reach length of more than 30 years, and retrieval algorithms deliver increasingly accurate results. This offers a great opportunity to get a spatial view of well-known parameters and to supplement station data. There are several hundreds of stations worldwide with sunshine duration observations on climatological time scales. Each of these stations has its own representativeness, instrument features and changes in instrumentation or location characteristics. To analyze sunshine duration on climatological time scales, all these features have to be considered. This is difficult for one station—and it is much more difficult for hundreds of stations—to get a spatial overview. This is one example where satellite-based data can supplement climate studies. For instance, a satellite-based climate data record of 30 years length for the Meteosat disk is usually based on about ten more-or-less identical instruments with very well known characteristics. This offers the opportunity to do climate studies for large regions with one single dataset of spatial and temporal homogeneous data.

There are several studies to derive sunshine duration from satellite observations. For instance, Kandirmaz [3] used a statistical relationship between the daily mean cloud cover index and measured sunshine duration to derive daily global sunshine duration from geostationary satellite data.

Kandirmaz [3] tested this method on data from the Meteosat First Generation (MFG). Good [4] used 15-minutes time series of cloud type data from Meteosat Second Generation (MSG) to compute daily sunshine duration for the United Kingdom. Shamim et al. [5] modeled sunshine duration with the help of geostationary satellite images for the United Kingdom. Journée et al. [6] derived sunshine duration maps for Belgium and Luxembourg from MFG global and direct solar radiation using the Ångström–Prescott equation [7,8]. In a study by Kothe et al. [9] the method used by Good [4] was extended to Europe. Additionally, Kothe et al. [9] derived sunshine duration from MSG-based solar surface incoming direct radiation by using the WMO threshold of 120 W/m^2 for bright sunshine [10]. Both approaches were tested for one year of MSG-based data. Wu et al. [11] used cloud classification data from geostationary satellite data to estimate sunshine duration for a region in China.

Most of these studies tested their approaches either for a small region or for a short time period. Journée et al. [6] applied their method to 11 years of MFG-based data, but only for Belgium and Luxembourg. Kothe et al. [9] derived sunshine duration for the whole of Europe, but just for one year. Methods by Kandirmaz [3], Shamim et al. [5] or Wu et al. [11] additionally used station data from a limited region for training or regression. Thus, none of these studies could answer the question of the applicability of these approaches to regions on continental scale and on climatological time scales at the same time.

The significance of satellite-based solar radiation data for the evaluation of climate models has been recognized over the last few years (e.g., [12–15]). Compared to global radiation, there are many more stations worldwide that provide sunshine duration measurements. This could also increase the importance of sunshine duration for the climate modeling community. Another important scientific field of sunshine duration applications is in the field of agriculture (e.g., [16]) and vegetation (e.g., [17,18]).

In this study, the retrieval technique by Kothe et al. [9] will be applied in an advanced version for a time period of 33 years and for the whole Meteosat disk, including Europe, Africa and parts of South America. The daily and monthly sunshine duration data will be evaluated against station data to get an estimate of the accuracy and temporal stability. The resulting sunshine duration product is part of the SARAH-2 climate data record, which is provided free of charge by the EUMETSAT Satellite Application Facility on Climate Monitoring (CM SAF). The CM SAF (www.cmsaf.eu) is part of a network of Satellite Application Facilities, which is operated by the European Organisation for the Exploitation of Meteorological Satellites (EUMETSAT). The CM SAF, led by the Deutscher Wetterdienst (DWD), is deriving climate data records from geostationary and polar-orbiting satellite instruments.

Sections 2 and 3 give a description of the applied data and retrieval methods. An evaluation of the daily and monthly satellite-based sunshine duration compared to station-based data is shown in Section 4. The results of these comparisons and possible deficiencies are discussed in Section 4. The'final two sections present some examples and a conclusion.

2. Data

2.1. SARAH-2

The CM SAF provides a climate data record of solar surface radiation, called SARAH (Surface Solar Radiation Data Set—Heliosat). The second release of this climate data record (SARAH-2) is published free of charge via the CM SAF web user interface (wui.cmsaf.eu) [19]. SARAH-2 includes the parameters Effective Cloud Albedo (CAL), Surface Incoming Shortwave radiation (SIS), Surface Direct Irradiance (SDI), Spectrally Resolved Irradiance (SRI) and Sunshine Duration (SDU). The SDI includes two direct radiation products, the Surface Incoming Direct radiation (SID) and the Direct Normalized Irradiance (DNI), which is the basis for the retrieval of SDU. To derive SARAH-2 surface radiation parameters, the Heliosat algorithm is used [20]. SARAH-2 data are based on the MVIRI (Meteosat Visible and InfraRed Imager) and SEVIRI (Spinning Enhanced Visible and Infrared Imager) instruments onboard EUMETSAT's Meteosat satellites of the first and second generation. The retrieval

of CAL is based on the MVIRI broadband channel (0.45 to 1 μm) and an artificial SEVIRI broadband channel, which is derived by the two visible channels centered at 0.6 and 0.8 μm. The Heliosat method offers the opportunity to derive a continuous dataset of CAL from a combination of MVIRI and SEVIRI measurements. For that, Heliosat includes an integrated self-calibration parameter that minimizes the impacts of satellite changes and artificial trends due to degradation of satellite instruments [21].

The first step in the Heliosat method is the retrieval of CAL by using the normalized relation between all sky and clear sky reflection in the visible channel of the Meteosat instruments. CAL is used to derive the cloud index, which is a measure for the impact of clouds on the clear-sky irradiance. The clear-sky irradiance is calculated using the all sky model SPECMAGIC [22]. Then a combination of cloud index and clear-sky irradiance gives SIS. SID is derived using the diffuse model of Skartveit et al. [23] and the cloud index. The direct normalized irradiance, DNI, is derived from SID by normalization with the cosine of the solar zenith angle (SZA):

$$DNI = \frac{SID}{\cos(SZA)} \tag{1}$$

A detailed description of the retrieval of SARAH surface radiation parameters can be found in Mueller et al. [24] and the ATBD [25]. SARAH radiation parameters were investigated in several publications [26–29]. The CM SAF validation report shows for SARAH-2 DNI a mean absolute difference of 33.4 W/m^2 for daily averages and 16.4 W/m^2 for monthly averages in comparison with station data from the Baseline Surface Radiation Network (BSRN) [30].

2.2. Station-Based Sunshine Duration Data

For the evaluation of sunshine duration, data from the European Climate Assessment & Datasets (ECA&D) and CLIMAT observation station network were used in this study. ECA&D [31] is gathering long-term daily observational series from meteorological stations all over Europe. Some automatic quality control and homogeneity checks are applied to the data. The sunshine duration has to be between 0 and 24 h, otherwise it is flagged as suspect [32]. Only ECA&D data were used, which were available in a predefined time subset from 1979 to 2016. Due to some national restrictions, only a part of the ECA&D data is downloadable. In contrast, the main application for CLIMAT [33] data is climate analysis and these data are therefore monthly totals. CLIMAT is a collection of monthly climate reports of more than 2.500 stations worldwide. The CLIMAT data undergo routine quality control at DWD. This includes an automatic comparison with long-term means and the percentage of sunshine duration (if these values are known), and a manual check for values, which were flagged as problematic. As no tests for homogeneity are applied for CLIMAT sunshine duration data, additionally some basic visual checks were applied to extract suspicious stations with obvious jumps or breaks in the time series. Only CLIMAT stations with at least 120 months of data were used for evaluation purposes. The metadata, which are provided by ECA&D and CLIMAT, give no information about the type of instrument or artificial changes, such as relocations or instrument changes. Since the 1980s, several national meteorological services changed from instruments, such as Campbell-Stokes, to automatic sunshine duration recorders [34]. This change can introduce inhomogeneities in the time series, which are not documented for all cases [35–38]. CLIMAT and ECA&D sunshine duration data are only available for land-based stations. ECA&D and CLIMAT station data are available for a relatively large number of stations, but despite quality checks, there is no guarantee that these data are bias free. Stations were removed from the analysis if they reported apparently erroneous data, such as fixed zeros, permanently high values throughout the year or obvious jumps in the time series. CLIMAT data were accessed via the DWD Climate Data Centre.

3. Approach

Basis for the retrieval of satellite-based SDU are the SARAH-2 30 min instantaneous DNI data and the World Meteorological Organization (WMO) threshold for bright sunshine, which is defined by

DNI $\geq$ 120 W/m^2. Daily SDU is derived using the ratio of Meteosat observations (slots) exceeding the DNI threshold, and hence are considered as sunny slots, to all slots during daylight:

$$SDU = daylength \times \frac{\sum_{i=1}^{\#daylight\ slots} W_i}{\#daylight\ slots} \qquad (2)$$

The day length is calculated depending on the date, longitude and latitude. The day length is restricted by a threshold of the solar elevation angle (SEA) of 2.5° [9]. W_i is a number between 0 and 1, which indicates the influence of a single slot depending on the number of surrounding cloudy and sunny grid points. The derivation of W_i is discussed in more detail in Section 3.1. The number of daylight slots (#daylight slots) describes the maximum number of Meteosat observations per grid point and per day during daylight. Daylight is defined by the time where the SEA exceeds 2.5°.

3.1. Weighting of Sunny Slots

A grid point at a specific time slot *i* is regarded as sunny if DNI is 120 W/m^2 or larger (see Equation (3)). SARAH-2 provides instantaneous DNI data every 30 min. Therefore, without weighting, in Equation (2) one sunny slot would correspond to a 30 min time window. In reality this is only the case in bright weather situations. If there are clouds in the surrounding area of a grid point, there is a probability that not the whole 30 min are sunny. This is also valid in the opposite case, when a cloudy grid point has sunny grid points in its near surroundings. This fact is accounted for in the retrieval of SDU by using the information of the 24 surrounding grid points (see Figure 1). In addition the information of two successive time steps is incorporated.

$$SIn_i = \begin{cases} \mathbf{1}\ if\ DNI(x,y) \geq \mathbf{120\ W/m^2} \\ \mathbf{0}\ if\ DNI(x,y) < \mathbf{120\ W/m^2} \end{cases} \qquad (3)$$
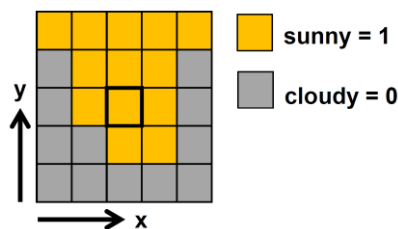
Figure 1. Demonstration for accounting for surrounding grid points. The target grid point is marked in the center.

In a first step for each grid point the number of sunny grid points in an environment of 24 grid points plus the center grid point is summed up (see Equation (4)).

$$\#SIn_i(x,y) = \sum_{m=y-2}^{m=y+2}\sum_{n=x-2}^{n=x+2} SIn_i(m,n) \qquad (4)$$

This is done for each daytime slot *i*. The number of each time step is combined with the number of the previous time step for each pixel to incorporate also the temporal shift of clouds in a simplified way (see Equation (5)).

$$\begin{aligned} N_1 &= \# SIn_1 \times 0.04 \\ N_i &= (\# SIn_i + \# SIn_{i-1}) \times 0.02 \end{aligned} \qquad (5)$$

By using a factor of 0.04 (in case of *i* = 1) or 0.02 (*i* > 1) the resulting number *N* is 1 in case that all 25 grid points are sunny, and 0 in the case that no grid point is sunny.

In a second step the impact of cloudy and sunny grid points on the temporal length of one time slot is estimated. The fraction of time, which slot *i* contributes to the daily SDU is derived by Equation (6):

$$W_i = \begin{cases} \max(N_i, C1) \, if \, DNI(Cgp) \geq 120 \, \text{W/m}^2 \\ N_i \cdot C2 \, if \, DNI(Cpg) < 120 \, \text{W/m}^2 \end{cases} \tag{6}$$

If at the center grid point (Cgp) DNI $\geq$ 120 W/m^2, the grid point is regarded as sunny, and W_i is equal to N_i, but not smaller than *C1*. If at Cgp DNI < 120 W/m^2 W_i is the product of N_i and *C2*.

The constants *C1* and *C2* are derived empirically by sensitivity tests, where the bias compared to reference station data in Germany was minimized. *C1* is set to 0.4 and indicates the minimum fraction that a single sunny slot can contribute. *C2* is set to 0.05 and defines the weight for the contribution of a non-sunny slot. The final SDU in hours is then derived by Equation (2).

4. Evaluation Results

The uncertainty of SDU was estimated in comparison to station-based sunshine duration measurements from ECA&D and CLIMAT (see Section 2.2). Depending on the data availability ECA&D data were used as reference for comparisons of daily SDU and CLIMAT data were used as reference for comparisons of monthly SDU. Measures for the accuracy are the bias, mean absolute difference (MAD) and the correlation following Pearson. A detailed evaluation of SARAH-2 SDU for the UK against gridded station data is available by Zeder et al. [39]. Bias, MAD and Pearson correlation *r* were calculated as follows:

$$Bias = \frac{1}{n} \sum_{i=1}^{n} (SDU_{SARAH_i} - SDU_{Station_i})$$

$$MAD = \frac{1}{n} \sum_{i=1}^{n} |SDU_{SARAH_i} - SDU_{Station_i}|$$

$$r = \frac{\sum_{i=1}^{n} (SDU_{SARAH_i} - \overline{SDU_{SARAH}})(SDU_{Station_i} - \overline{SDU_{Station}})}{\sqrt{\sum_{i=1}^{n} (SDU_{SARAH_i} - \overline{SDU_{SARAH}})^2} \cdot \sqrt{\sum_{i=1}^{n} (SDU_{Station_i} - \overline{SDU_{Station}})^2}}$$

### 4.1. Evaluation of Daily Data

For the comparison of daily SDU only ECA&D stations with data between 1983 and 2015 were chosen. All CM SAF SDU files contain information about the number of available slots per day. As the uncertainty of SDU increases with decreasing number of available slots per day, only days with 24 or more slots were used for the comparison with ECA&D data. The CM SAF SARAH-2 SDU climate data record contains 12,028 days with SDU data and 11,911 days were derived from 24 or more available slots per day. The reasons for missing slots were mainly maintenances or failures of the satellite instrument or data storage issues. Most of the missing slots were in the operation time of Meteosat 2 (till 1988).

The comparison of SDU and ECA&D daily sunshine duration measurements showed a positive bias of 0.41 h (Table 1). Figure 2 shows that the found biases are lowest in Germany, which might be partly due to the determination method for the constants *C1* and *C2*. Higher biases were found in Spain and especially on the Balearic and Canary Islands. The highest seasonal bias was in the months September to November (SON) with 0.53 h.

Table 1 shows for the comparison of daily SDU and ECA&D a MAD of 1.33 h. The lowest MAD values were found in northern Germany (Figure 3). The MAD was highest in the Alpine region, northern Spain and the Canary Islands. In the summer season (June to August, JJA) the MAD is a little higher with 1.43 h, which is probably due to the higher absolute SDU values in this season.

Table 1. Bias, MAD and correlation for the comparison of daily SDU and ECA&D for the time period 1983–2015. The mean includes 2,472,762 compared daily values. Seasons are divided into March to May (MAM), June to August (JJA), September to November (SON) and December to January (DJF).

|	Bias (h)	MAD (h)	Correlation
Mean	0.41	1.33	0.91
MAM	0.32	1.38	0.92
JJA	0.41	1.43	0.93
SON	0.53	1.26	0.88
DJF	0.37	1.23	0.81
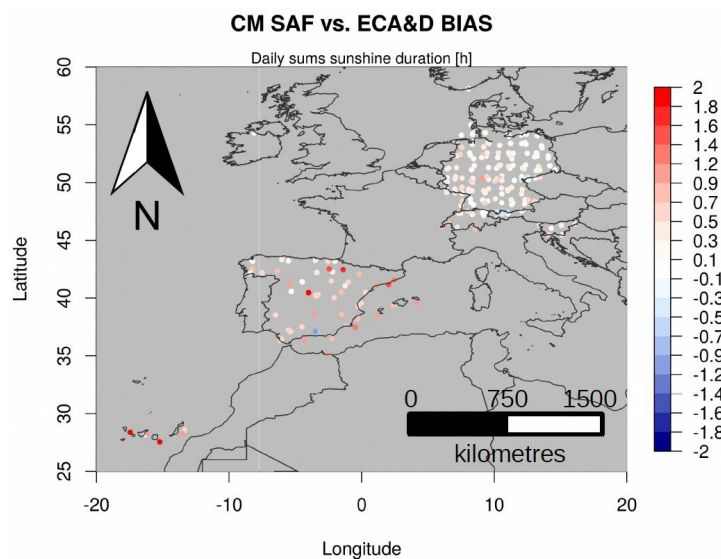
Figure 2. Spatial distribution of the bias (h) between daily SDU and ECA&D for the time period 1983 to 2015.
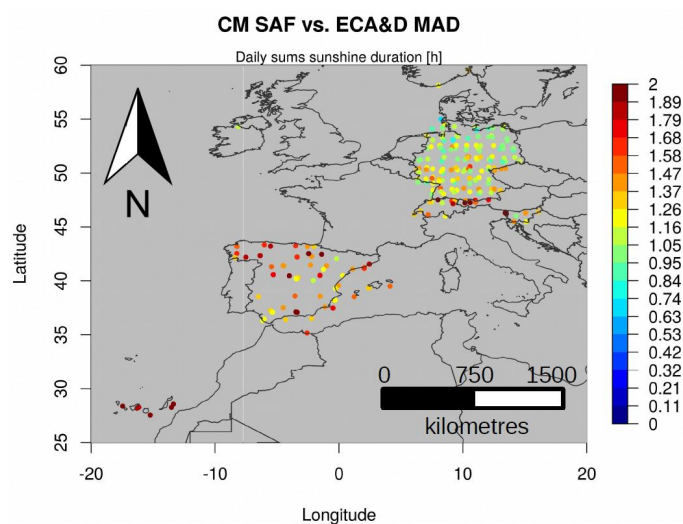
Figure 3. Spatial distribution of the MAD (h) between daily SDU and ECA&D for the time period 1983 to 2015.

The correlation between SDU and ECA&D is high with 0.91 (Table 1), but shows a lower value of 0.81 in winter (December to February, DJF). Figure 4 shows the temporal evolution of the normalized bias in SDU. This figure illustrates that the bias is very stable in time and has no significant trend.
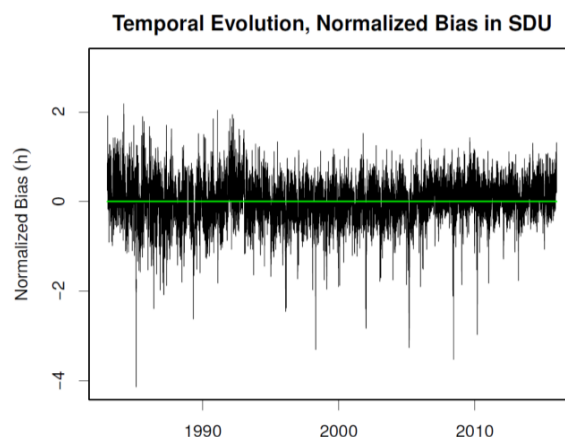
Figure 4. Temporal evolution of the normalized bias (h) between daily SDU and ECA&D for the time period 1983 to 2015. The normalized bias is the mean value for all stations.

4.2. Evaluation of Monthly Data

The evaluation of monthly sums of SDU was done with reference to measurements of CLIMAT ground stations. A requirement to the chosen CLIMAT stations was the availability of at least ten years of data between 1983 and 2015. To account for some missing days of SDU the monthly sum of SDU was derived by multiplying the monthly mean SDU with the number of days per month. There are 18 missing days in the time period from 1983 to 1991, most of them (6) in 1983.

The comparison of monthly sums of SDU against CLIMAT data showed a good agreement with a positive bias of 7.5 h (Table 2). The spatial distribution of the bias shows much higher bias values in West Africa with partly more than 50 h overestimation of SDU compared to CLIMAT (Figure 5). There is also some seasonal variation in the bias with the highest value from September to November (SON) of 10.3 h (Table 2). However, as the CLIMAT stations are heterogeneously distributed on the northern and southern hemisphere, the seasonal variation is difficult to interpret. To see the seasonal impact on SDU differences, Table 2 shows the bias and MAD divided by stations north of 23°N (NH) and south of 23°S (SH). The bias on the NH varies between 4.7 h from March to May (MAM) and 10.3 h for SON and on the SH between 0.9 h for DJF and −3.8 h for SON.
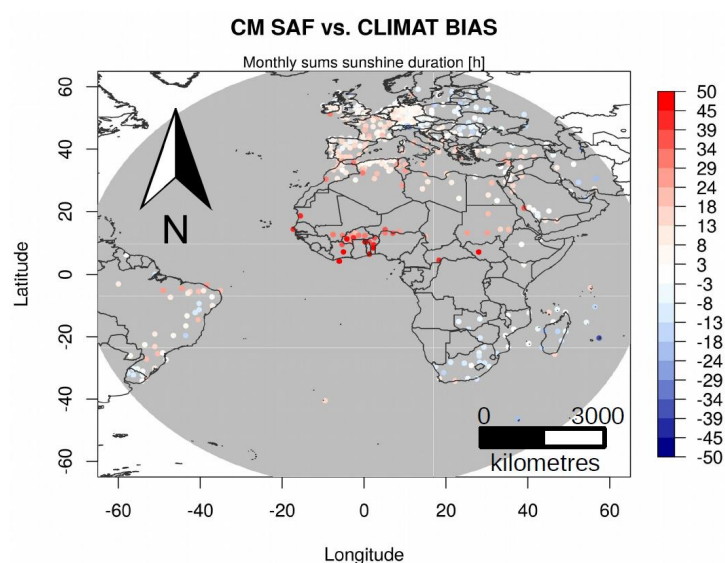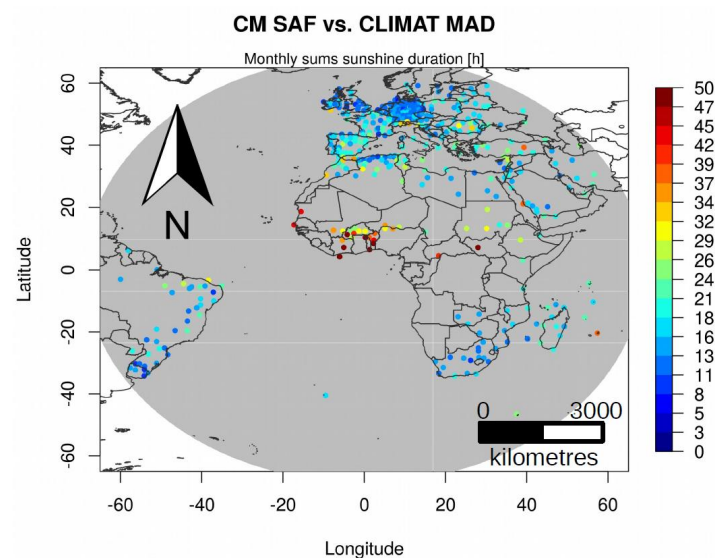

Figure 5. Spatial distribution of the bias (h) between monthly SDU and CLIMAT for the time period 1983 to 2015.

Table 2. Bias, MAD and correlation for the comparison of daily SDU and CLIMAT for the time period 1983–2015. The mean includes 117.933 compared monthly values. The Northern Hemisphere (NH) is defined by latitude >23°, the Southern Hemisphere (SH) by latitude <−23°. Seasons are divided into March to May (MAM), June to August (JJA), September to November (SON) and December to January (DJF).

	Bias (h)	MAD (h)	Correlation
Mean	7.5	18.4	0.96
Mean NH	6.4	17.4	0.97
Mean SH	−2.2	15.2	0.95
MAM	7.8	20.1	0.92
MAM NH	4.7	18.6	0.94
MAM SH	−0.4	14.6	0.95
JJA	8.6	20.6	0.93
JJA NH	6.9	20.5	0.93
JJA SH	−3.2	13.6	0.97
SON	10.3	18.0	0.96
SON NH	10.3	17.0	0.97
SON SH	−3.8	15.0	0.95
DJF	9.1	20.2	0.96
DJF NH	6.8	18.5	0.94
DJF SH	0.9	17.6	0.93

The MAD is 18.4 h (Table 2). As the long-term mean of SDU monthly sums for the whole Meteosat disk is about 215 h, this results in an uncertainty of less than nine percent (18.4 h/215 h = 8.6%). The spatial distribution of MAD (Figure 6) shows the highest uncertainties in West Africa. The seasonal variation of MAD is between 18.0 h for SON to 20.6 h for JJA. For the NH the MAD is highest (20.5 h) for JJA and lowest (17.0 h) for SON, while for the Southern Hemisphere there is a MAD of 17.6 h for DJF and 13.6 h for JJA.


Figure 6. Spatial distribution of the MAD (h) between monthly SDU and CLIMAT for the time period 1983 to 2015.

The correlation coefficient between SDU and CLIMAT monthly sums is very high with 0.96 (Table 2). This value is even higher than for the daily evaluation against ECA&D and has only minor variations throughout the seasons. The temporal evolution of the normalized bias (Figure 7) shows only a very low positive trend, which is not significant. The graph (Figure 7) illustrates that the SDU

time series is stable, but there is a conspicuous peak in 1992 and an increase after 2005, which have to be evaluated.
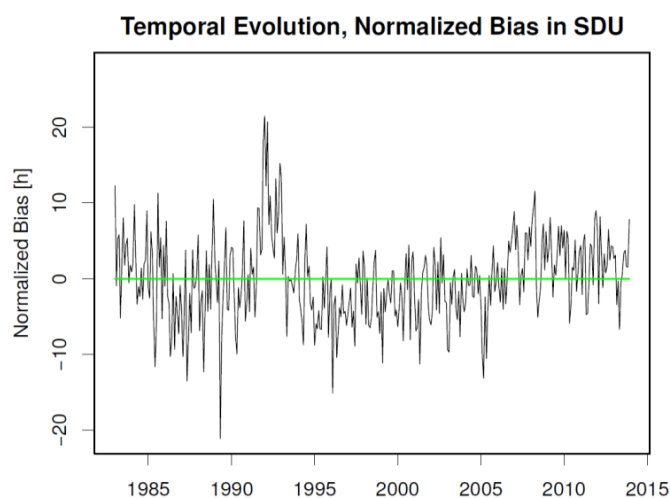
Figure 7. Temporal evolution of the normalized bias (h) between monthly SDU and CLIMAT for the time period 1983 to 2015. The normalized bias is the mean value for all stations.

4.3. Discussion

Overall the comparisons of SDU against ECA&D and CLIMAT station-based data show a good agreement, with small uncertainty and high correlation. Compared to other surface radiation parameters there are a high number of station-based measurements for sunshine duration available. Nevertheless, there is no information about the quality of individual ECA&D and CLIMAT sunshine duration time periods. Even after manual inspection and some basic automated quality checks there is an unknown uncertainty for these station data.

Another issue regarding the comparison of satellite-based and station-based data is the representativeness of each station for a satellite pixel of the size of $0.05° \times 0.05°$. This issue can explain some higher uncertainties in mountainous areas or islands. Mountain summits, where stations usually are placed, can influence the surrounding clouds, which is visible in the satellite pixel, but not in the station data. Shadowing of stations is also relevant, as this is not considered in the satellite-based data. For instance, the comparison of daily SDU shows for Spain a strong variation of the bias over short distances, which is unlikely due to small-scale variations in the satellite-based SDU.

The correlation of daily SDU against ECA&D shows a decrease in winter. As ECA&D stations are all in the northern hemisphere (mainly in Germany and Spain) the lower correlation values for DJF might be due to snow cover. Snow cover can be misinterpreted by satellite retrievals (see Section 2.1) as clouds. This leads to an underestimation of solar surface radiation and accordingly to an underestimation of SDU. In addition, the uncertainty of the ground station measurements increases in the case of snow, because regular maintenance of the instruments is needed.

Higher uncertainties in West Africa can be explained by an issue with low clouds. Hannak et al. [40] showed that in the region of West Africa there are large and persistent low cloud fields. They postulated that the self-calibrating method of the Heliosat algorithm leads to an underestimated effective cloud albedo in the region with persistent cloud cover, since the scenes with minimum number of counts are still contaminated with clouds [40]. This leads to a strong overestimation of surface radiation and SDU in this area. In addition, this effect could be reinforced by an underestimation of aerosols optical depth (AOD). In the retrieval of SARAH-2 a constant AOD climatology was used. Thus, biomass burning or dust outbreaks are not regarded in the retrieval and can lead to the observed overestimation of surface radiation.

The Figures 4 and 7 confirm that the daily and monthly SDU time series are very stable from 1983 to 2015. There is a peak after 1991, which is very likely due to the Pinatubo eruption in June 1991. The constant AOD climatology of the SARAH-2 retrieval might be the reason why the SARAH-2 data record does not include the effects of the Pinatubo eruption, which reduced the solar radiation up to three years after the event. Thus, SDU is reduced in station data, but not in SARAH-2 SDU, which leads to an overestimation during that time. Figure 7 shows a slight increase in the normalized SDU bias after 2005, which might be attributed to the change from the Meteosat MVIRI to the SEVIRI instruments. The transition between MVIRI and SEVIRI as well as the implementation of improved aerosols will be further investigated for future SARAH releases.

An issue that might have an influence on the results of the evaluation in some regions is artificial patterns, which are most obvious in cloud-free areas with a high solar insolation, such as deserts. These artifacts are a result of the combination of 30 min instantaneous data, where the threshold of $DNI \geq 120 \, W/m^2$ is already reached at the twilight zone. Figure 8 shows an example of daily SDU, where artificial patterns are visible in the Kalahari and Sahara deserts. These spatial jumps of SDU can be up to 30 min differences, which may have a slight impact on the results of the comparisons in Section 4.2. For longer sampling periods, such as monthly averages or monthly sums of SDU, these patterns disappear.
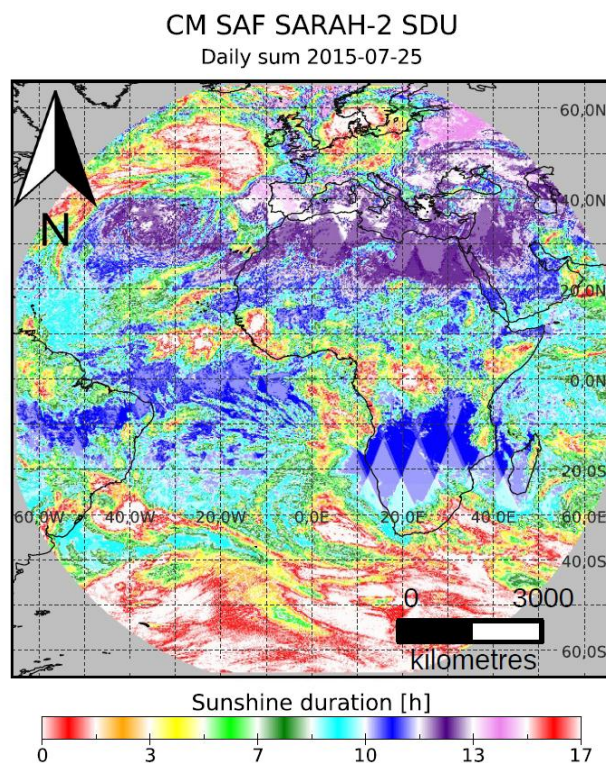
Figure 8. Daily sum SDU (h) for 25 July 2015. The colorbar highlights artificial patterns in Africa.

5. Applications

Figure 9 shows the mean annual sum of SDU for 1983 to 2015 for different regions. This figure also demonstrates that the high spatial resolution of $0.05° \times 0.05°$ is suitable for many applications from continental to local scales. The main impacts on sunshine duration are atmospheric parameters, such as clouds, water vapor and aerosols. However, also topographic features and local processes influence SDU and can be seen in Figure 9. For instance the gradient in SDU between the northern and southern side of the Alps or the Pyrenees is a good example for the blocking impact of these mountain ranges.
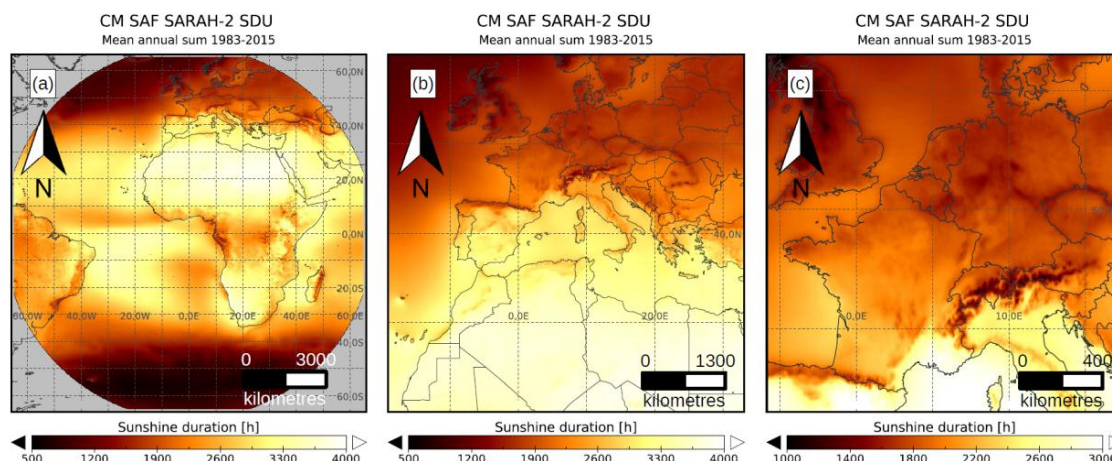
Figure 9. Mean annual sum (h) of SDU for the time period 1983 to 2015 for the Meteosat disk (**a**), Europe and North Africa (**b**), and Central Europe (**c**).

Trend in Sunshine Duration

The temporal coverage of 33 years and the temporal stability of the data allow climatological investigations. For instance, trend analysis can be a valuable tool to investigate impacts of a changing climate. Figure 10 shows the linear decadal trend for SDU. Except for some regions in the tropics, the decadal trend in SDU for 1983 to 2015 (Figure 10a) is slightly positive or around zero. Significant trends were found mainly south of the equator. A split of the time series from 1983 to 1999 and 2000 to 2015 shows very different trend patterns (Figure 10b,c). In many regions the found trends were even opposite. For instance, there is a strong positive trend from 2000 to 2015 in Eastern Europe, while there is a slightly negative trend in this region from 1983 to 1999. There is a positive trend in the Atlantic Ocean near the Canary Islands from 1983 to 1999, while there is a slightly decreasing trend in this region from 2000 to 2015. A study by Pfeifroth et al. [41] shows that trends of SARAH-2 surface radiation are slightly underestimated compared to the corresponding trends of station-based surface radiation data. A possible reason for this underestimation of trends is the usage of constant AODs. Thus, most of the found trends in SARAH-2 SDU are due to changes in clouds and water vapor. Nevertheless, the found trends are comparable to trends in solar radiation, which were recently investigated by Arturo Sanchez-Lorenzo et al. [42], Alexandri et al. [29] and Pfeifroth et al. [41] for European station data.
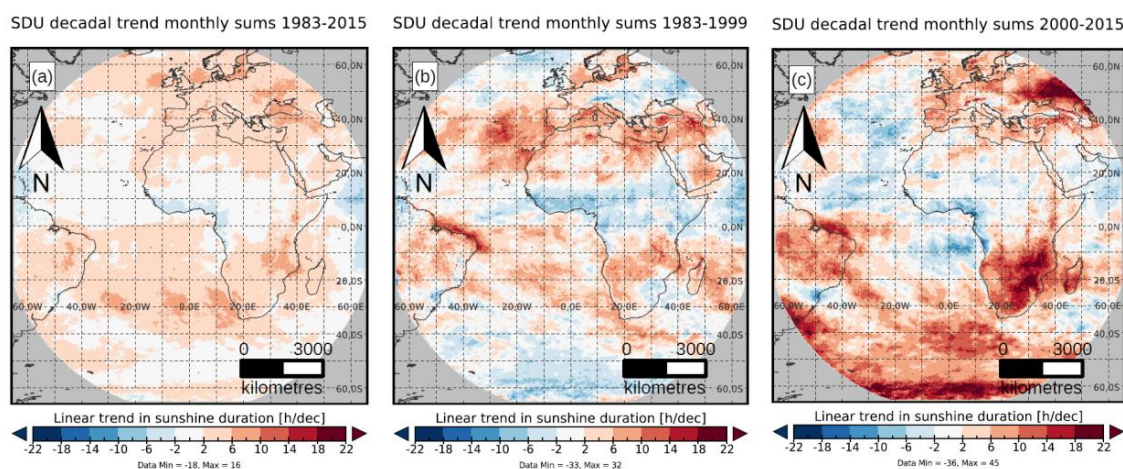
Figure 10. Linear decadal trend in SDU for the time period 1983 to 2015 (**a**), 1983 to 1999 (**b**), 2000 to 2015 (**c**).

6. Conclusions

The CM SAF SARAH-2 SDU is the first climate data record for daily and monthly sunshine duration covering Europe, Africa and parts of South America for the time period 1983 to 2015. The retrieval is based on the WMO threshold for sunshine of DNI $\geq$ 120 W/m^2 and additionally estimates the impact of surrounding grid points. SARAH-2 SDU has a spatial resolution of $0.05° \times 0.05°$ and is therefore highly suitable for regional analysis. The comparison against daily ECA&D station-based measurements showed a good agreement with a bias of 0.41 h, a MAD of 1.31 h and a correlation of 0.91. The highest MADs were found in mountainous regions and on islands, which might be an issue of representativeness. In comparison with CLIMAT station-based monthly sums of sunshine duration, the CM SAF SDU slightly overestimated the sunshine duration. The evaluation against CLIMAT gave a bias of 7.5 h, MAD of 18.4 h and a correlation of 0.96. Thus, the uncertainty of SDU compared to CLIMAT is well below 9% in most regions of the Meteosat disk. Besides the high accuracy of SDU it was shown that the time series is very stable.

There are still some deficiencies, such as minor artifacts in some scenes, an issue with low clouds in West Africa, a constant AOD climatology or cases of a misinterpretation of snow coverage as clouds, which will be investigated for a next version.

The CM SAF SARAH-2 SDU climate data record is freely available via wui.cmsaf.eu. The combination of a well-known meteorological parameter with high-quality, high spatial resolution for a homogeneous time series of 33 years is qualified for many climate applications, including variability and trend analysis. For instance, the combination of SARAH-2 SDU and station-based data by merging could be a highly beneficial application for the near future.

Author Contributions: Steffen Kothe designed and performed the study and analyzed the data. Uwe Pfeifroth and Jörg Trentmann contributed SARAH-2 DNI data and gave feedback. Roswitha Cremer supported the data analysis. Rainer Hollmann is the scientific manager of the project and gave feedback.

Conflicts of Interest: The authors declare no conflict of interest.

References

1. Pallé, E.; Butler, C.J. Sunshine records from Ireland: Cloud factors and possible links to solar activity and cosmic rays. *Int. J. Climatol.* **2001**, *21*, 709–729. [CrossRef]
2. Founda, D.; Kalimeris, A.; Pierros, F. Multi annual variability and climatic signal analysis of sunshine duration at a large urban area of Mediterranean (Athens). *Urban Clim.* **2014**, *10*, 815–830. [CrossRef]
3. Kandirmaz, H.M. A model for the estimation of the daily global sunshine duration from meteorological geostationary satellite data. *Int. J. Remote Sens.* **2006**, *27*, 5061–5071. [CrossRef]
4. Good, E. Estimating daily sunshine duration over the UK from geostationary satellite data. *Weather* **2010**, *65*, 324–328. [CrossRef]
5. Shamim, M.A.; Remesan, R.; Han, D. An improved technique for global daily sunshine duration estimation using satellite imagery. *J. Zhejiang Univ. Sci.* **2012**, *13*, 717–722. [CrossRef]
6. Journée, M.; Demain, C.; Bertrand, C. Sunshine duration climate maps of Belgium and Luxembourg based on Meteosat and in-situ observations. *Adv. Sci. Res.* **2013**, *10*, 15–19. [CrossRef]
7. Ångström, A. Solar and terrestrial radiation. *Q. J. R. Meteorol. Soc.* **1924**, *50*, 121–125.
8. Prescott, J.A. Evaporation from water surface in relation to solar radiation. *Trans. R. Soc. Aust.* **1940**, *64*, 114–125.
9. Kothe, S.; Good, E.; Obregón, A.; Ahrens, B.; Nitsche, H. Satellite-based sunshine duration for Europe. *Remote Sens.* **2013**, *5*, 2943–2972. [CrossRef]
10. World Meteorological Organization (WMO). *Guide to Meteorological Instruments and Methods of Observation*, 7th ed.; WMO: Geneva, Switzerland, 2008.

11. Wu, B.; Liu, S.; Zhu, W.; Yu, M.; Yan, N.; Xing, Q. A method to estimate sunshine duration using cloud classification data from a geostationary meteorological satellite (FY-2D) over the Heihe River Basin. *Sensors* **2016**, *16*, 1859. [CrossRef] [PubMed]

12. Kothe, S.; Dobler, A.; Beck, A.; Ahrens, B. The radiation budget in a regional climate model. *Clim. Dyn.* **2011**, *36*, 1023–1036. [CrossRef]

13. Katragkou, E.; García-Díez, M.; Vautard, R.; Sobolowski, S.; Zanis, P.; Alexandri, G.; Cardoso, R.M.; Colette, A.; Fernandez, J.; Gobiet, A.; et al. Regional climate hindcast simulations within EURO-CORDEX: Evaluation of a WRF multi-physics ensemble. *Geosci. Model Dev.* **2015**, *8*, 603–618. [CrossRef]

14. Chiacchio, M.; Solmon, F.; Giorgi, F.; Stackhouse, P.; Wild, M. Evaluation of the radiation budget with a regional climate model over Europe and inspection of dimming and brightening. *J. Geophys. Res.* **2015**, *120*, 1951–1971. [CrossRef]

15. Alexandri, G.; Georgoulias, A.K.; Zanis, P.; Katragkou, E.; Tsikerdekis, A.; Kourtidis, K.; Meleti, C. On the ability of RegCM4 regional climate model to simulate surface solar radiation patterns over Europe: An assessment using satellite-based observations. *Atmos. Chem. Phys.* **2015**, *15*, 13195–13216. [CrossRef]

16. Murthy, V.R.K. Crop growth modeling and its applications in agricultural meteorology. *Satell. Remote Sens. GIS Appl. Agric. Meteorol.* **2011**, *1*, 235–261.

17. Wang, L.; Gong, W.; Ma, Y.; Zhang, M. Modeling regional vegetation NPP variations and their relationships with climatic parameters in Wuhan, China. *Earth Interact.* **2013**, *17*, 1–20. [CrossRef]

18. Wang, H.; Liu, D.; Lin, H.; Montenegro, A.; Zhu, X. NDVI and vegetation phenology dynamics under the influence of sunshine duration on the Tibetan plateau. *Int. J. Climatol.* **2015**, *35*, 687–698. [CrossRef]

19. Pfeifroth, U.; Kothe, S.; Müller, R.; Cremer, R.; Trentmann, J.; Hollmann, R. Surface solar radiation data set—Heliosat (SARAH)—Edition 2. *Satell. Appl. Facil. Clim. Monit.* **2017**. [CrossRef]

20. Hammer, A.; Heinemann, D.; Hoyer, C.; Kuhlmann, R.; Lorenz, E.; Müller, R.; Beyer, H.G. Solar energy assessment using remote sensing technologies. *Remote Sens. Environ.* **2003**, *86*, 423–432. [CrossRef]

21. Mueller, R.; Trentmann, J.; Träger-Chatterjee, C.; Posselt, R.; Stöckli, R. The Role of the effective cloud albedo for climate monitoring and analysis. *Remote Sens.* **2011**, *3*, 2305–2320. [CrossRef]

22. Mueller, R.; Behrendt, T.; Hammer, A.; Kemper, A. A New algorithm for the satellite-based retrieval of solar surface irradiance in spectral bands. *Remote Sens.* **2012**, *4*, 622–647. [CrossRef]

23. Skartveit, A.; Olseth, J.; Tuft, M. An hourly diffuse fraction model with correction for variability and surface albedo. *Sol. Energy* **1998**, *63*, 173–183. [CrossRef]

24. Mueller, R.; Pfeifroth, U.; Träger-Chatterjee, C.; Trentmann, J.; Cremer, R. Digging the METEOSAT treasure—3 decades of solar surface radiation. *Remote Sens.* **2015**, *7*, 8067–8101. [CrossRef]

25. CM SAF Algorithm Theoretical Baseline Document, Meteosat Solar Surface Radiation and effective Cloud Albedo Climate Data Records—Heliosat, SARAH-2 2017. Under Preparation. Available online: http://www.cmsaf.eu/EN/Documentation/Documentation/ATBD/ATBD_node.html (accessed on 1 May 2017).

26. Riihelä, A.; Thomas Carlund, T.; Trentmann, J.; Müller, R.; Lindfors, A.V. Validation of CM SAF surface solar radiation datasets over Finland and Sweden. *Remote Sens.* **2015**, *7*, 6663–6682. [CrossRef]

27. Žák, M.; Mikšovský, J.; Pišoft, P. CMSAF radiation data: New possibilities for climatological applications in the Czech Republic. *Remote Sens.* **2015**, *7*, 14445–14457. [CrossRef]

28. Loew, A.; Peng, J.; Borsche, M. High-resolution land surface fluxes from satellite and reanalysis data (HOLAPS v1.0): Evaluation and uncertainty assessment. *Geosci. Model Dev.* **2016**, *9*, 2499–2532. [CrossRef]

29. Alexandri, G.; Georgoulias, A.K.; Meleti, C.; Balis, D.; Kourtidis, K.A.; Sanchez-Lorenzo, A.; Trentmann, J.; Zanis, P. A high resolution satellite view of surface solar radiation over the climatically sensitive region of Eastern Mediterranean. *Atmos. Res.* **2017**, *188*, 107–121. [CrossRef]

30. CM SAF Validation Report, Meteosat Solar Surface Radiation and Effective Cloud Albedo Climate Data Record. Under Preparation. 2017. Available online: http://www.cmsaf.eu/EN/Documentation/Documentation/ValidationRep/ValidationReports_node.html (accessed on 1 May 2017).

31. Klein Tank, A.M.G.; Wijngaard, J.B.; Konnen, G.P.; Bohm, R.; Demaree, D.; Gocheva, A.; Mileta, M.; Pashiardis, S.; Hejklik, L.; Kern-Hansen, C.; et al. Daily dataset of 20th-century surface air temperature and precipitation series for the European climate assessment. *Int. J. Climatol.* **2001**, *22*, 1441–1453. [CrossRef]

32. ECA&D Project Team. Algorithm Theoretical Basis Document (ATBD). 2013. Available online: http://www.ecad.eu/documents/atbd.pdf (accessed on 10 March 2017). version 10.7.

33. Deutscher Wetterdienst. Global Climate Data. Available online: http://www.dwd.de/EN/ourservices/climat/climat.html (accessed on 9 March 2017).

34. Sanchez-Lorenzo, A.; Wild, M. Decadal variations in estimated surface solar radiation over Switzerland since the late 19th century. *Atmos. Chem. Phys. Discuss.* **2012**, *12*, 8635–8644. [CrossRef]

35. Legg, T. Comparison of daily sunshine duration recorded by Campbell-Stokes and Kipp and Zonen sensors. *Weather* **2014**, *69*, 264–267. [CrossRef]

36. Matuszko, D. A comparison of sunshine duration records from the Campbell-Stokes sunshine recorder and CSD$_3$ sunshine duration sensor. *Theor. Appl. Climatol.* **2015**, *119*, 401–406. [CrossRef]

37. Sanchez-Romero, A.; González, J.; Calbó, J.; Sanchez-Lorenzo, A. Using digital image processing to characterize the Campbell-Stokes sunshine recorder and to derive high-temporal resolution direct solar irradiance. *Atmos. Meas. Tech.* **2015**, *8*, 183–194. [CrossRef]

38. Van den Besselaar, E.J.M.; Sanchez-Lorenzo, A.; Wild, M.; Klein Tank, A.M.G.; de Laat, A.T.J. Relationship between sunshine duration and temperature trends across Europe since the second half of the twentieth century. *J. Geophys. Res. Atmos.* **2015**, *120*, 10823–10836. [CrossRef]

39. Zeder, J.; Good, E.; Kothe, S.; Trentmann, J. Comparison of in-situ and spaceborne derived monthly sunshine duration grids over the United Kingdom. Unpublished work. 2017.

40. Hannak, L.; Knippertz, P.; Fink, A.H.; Kniffka, A.; Pante, G. Why do global climate models struggle to represent low-level clouds in the West African summer monsoon? *Clim. Dyn.* **2016**. [CrossRef]

41. Pfeifroth, U.; Sanchez-Lorenzo, A.; Manara, V.; Trentmann, J. Trends and variability of surface solar radiation in Europe based on CM SAF satellite data records. *J. Geophys. Res.* **2017**, in press.

42. Sanchez-Lorenzo, A.; Enriquez-Alonso, A.; Wild, M.; Trentmann, J.; Vincente-Serrano, S.M.; Sanchez-Romero, A.; Posselt, R.; Hakuba, M. Trends in downward surface solar radiation from satellites and ground observations over Europe during 1983–2010. *Remote Sens. Environ.* **2017**. [CrossRef]